Conformational dynamics of a photosynthetic light-harvesting complex in native thylakoid membranes

Fatemeh Azadi-Chegeni[1]; Meaghan E. Ward[2]; Giorgio Perin[3]; Diana Simionato[3]; Tomas Morosinotto[3;] Marc Baldus[2]; Anjali Pandit[1,*]

[1] Leiden Institute of Chemistry, Dept. of Solid State NMR, Leiden University, Einsteinweg 55, 2333CC, Leiden, The Netherlands

[2] NMR Spectroscopy, Bijvoet Center for Biomolecular Research, Utrecht University, Padualaan 8, 3584 CH, Utrecht, The Netherlands

[3] PAR-Lab (Padua Algae Research Laboratory), Dept. of Biology, University of Padua, Via Ugo Bassi 58B, 35121 Padua, Italy

*corresponding author: a.pandit@chem.leidenuniv.nl

Keywords

In situ solid-state NMR, Light Harvesting Complex II (LHCII), N-terminal domain, non-photochemical quenching

Acknowledgements

AP and FA were financially supported by a CW-VIDI grant of the Netherlands Organization of Scientific Research (NWO) under grant nr. 723.012.103. We thank Emanuela Crisafi for assistance with the liposome preparations. MEW is a recipient of a Natural Sciences and Engineering Research Council of Canada Postdoctoral Fellowship. This work was supported in part by uNMR-NL, an NWO-funded National Roadmap Large-Scale Facility of the Netherlands (grant number: 184.032.207).

Abstract

Photosynthetic light-harvesting antenna complexes (LHCs) of plants, moss and green algae form dynamic switches between light harvesting and excitation-quenched, dissipative states. This mechanism protects the photosynthetic apparatus under light stress via a photo protective membrane response. Herein, we demonstrate the application of solid-state NMR spectroscopy to wild type, heterogeneous thylakoid membranes of *Chlamydomonas reinhardtii* (*Cr)* and purified *Cr* Light harvesting Complex II (LHCII) reconstituted in thylakoid lipid membranes, to detect the conformational dynamics of LHCII under native conditions. We find that membrane-reconstituted LHCII contains sites that undergo fast, large-amplitude motions, including the phytol tails of two chlorophylls. Furthermore, plasticity is observed in the N-terminal stretch and in the trans-membrane helical edges facing the thylakoid lumen. In intact thylakoids, the dynamics of these protein and pigment sites is significantly reduced. We conclude that LHCIIs contain flexible sites but that their conformational dynamics are constrained *in vivo*, implying that changes in the physicochemical environment are required to enable switching between different conformational states. *In situ* NMR spectroscopy opens a new route to investigate the plasticity of light-harvesting complexes and their seminal role in biological regulation mechanisms such as membrane state transitions, non-photochemical quenching or post-translational modifications.

Multi-pigment protein complexes in plants, moss, and photosynthetic algae perform delicate photo-physical and chemical tasks. These processes are highly regulated by the conformational flexibility of the proteins and their interplay within a dynamic thylakoid membrane environment [(1, 2)]. Obtaining atomic-level structures of these complexes under physiological conditions is an essential step towards understanding the molecular mechanisms that regulate the excitation energy flow. To understand the molecular mechanisms that regulate photosynthesis, the most abundant, peripheral antenna complex, Light Harvesting Complex II (LHCII), has been studied extensively and the conformational switch of LHCII has been the topic of much debate [(2-12)]. Single-molecule fluorescence studies have demonstrated that individual LHCII complexes can fluctuate between light harvesting and dissipative states [(4, 7)] and MD (Molecular Dynamics) simulations on LHCII in a lipid bilayer [(9)] suggest that the N-terminal region is highly disordered and could modulate excitation quenching. The conformational states and dynamics of LHCII have been previously investigated in crystals or detergent solutions [(4, 10, 13, 14)]. These conditions are very different from more native conditions where complexes are stabilized in a lipid bilayer and can interact with other proteins and lipids, which has been shown to affect their fluorescent states [(15, 16)]. Moreover, in native thylakoid membranes the antenna proteins are held in specific arrangements within LHCII-Photosystem II super complexes [(17)]. The presence of zeaxanthin, phase transitions and membrane stacking may further control the conformational dynamics of the individual LHCs [(18)], underlining the importance of studying their dynamic behavior in native surroundings.

Herein, we applied solid-state NMR (Nuclear Magnetic Resonance) spectroscopy to study the structure and dynamics of LHCII in native thylakoid membranes. Solid-state NMR spectroscopy has shown to be a powerful tool for atomistic detection of membrane proteins in native membrane or cellular environments and several *in-situ* and *in-cell* solid-state NMR studies have investigated membrane proteins that were overexpressed in prokaryotic and eukaryotic host-expression systems [(19-25)]. We take advantage of the fact that our target protein is present at a high natural abundance in thylakoid membranes under native conditions, and demonstrate that LHCII NMR signals can be detected in thylakoids isolated from wild-type eukaryotic *Chlamydomonas reinhardtii* (*Cr*) green algae cells. Isolated *U*-^{13}C,^{15}N *Cr* LHCII were analyzed that were reconstituted in thylakoid-lipid membranes, to

obtain a view on the conformational dynamics of LHCII in a lipid environment. By comparing these data to the spectra of native thylakoids, we uncover marked differences in the conformational dynamics of LHCII, with implications for the role of the thylakoid membrane environment for LHCII function.

Results and Discussion

Biochemical analysis of Cr *thylakoid membranes and of isolated* Cr *LHCII trimers*

The LHCII monomeric structure is characterized by three membrane-spanning helices (helix A-C) and two short helical fragments (helix D and E), the N- and C-tails, and segments containing large, water-exposed loops. Fig. 1(A-C) shows the protein structure, pigment-protein structure and a top view of the trimeric structure of LHCII. To investigate the occurrence of LHCII in the thylakoid preparation, we used the procedure described for the isolation of the LHCII trimers and ran a sucrose gradient. Fig. 1D clearly shows that the LHCII trimers are the most abundant pigment-containing complexes in the thylakoid preparations. Different molecular-weight bands are distinguished for LHCII in the SDS page analysis due to the fact that the LHCII trimers are isomers consisting of different polypeptides with different molecular weights. The most abundant polypeptides are Lhcbm1, Lhcbm2/7 (Lhcbm2 and Lhcbm7 have identical mature peptide sequences) and Lhcbm3 [(26)]. The absorbance spectrum of the thylakoid membranes confirms the presence of Chls and carotenoids (Fig. S1) and High Performance Liquid Chromatography (HPLC) data show that *Cr* LHCII proteins bind Chl*a* and *b*, lutein, neoxanthin or loroxanthin and violaxanthin, together with small traces of beta carotene and antheraxanthin [(27)].

NMR analysis of LHCII in lipid membranes: detection of resonance signals from protein, pigment and lipids

Two complementary types of solid-state NMR experiments were employed in this study that are selective for rigid, respectively highly dynamic, molecules. In cross-Polarization (CP) based experiments, ^{1}H-^{13}C or ^{13}C-^{15}N magnetization is transferred via dipolar interaction, which is dependent on the angle between an internuclear vector and the magnetic field.

Dipolar-based transfer experiments becomes inefficient for dynamic molecules, where the dipolar couplings are averaged to zero due to fast tumbling in solution. In INEPT based experiments, magnetization is transferred via *J* couplings. In the presence of strong motions, where orientation dependent interactions are sufficiently averaged out by magic-angle spinning and fast molecular tumbling, the combination of *J*-based pulse sequences can be employed for screening very flexible parts of large biomolecules [(28)]. Membrane proteins typically contain large transmembrane stretches with low flexibility, of which the majority of signals are detected in dipolar-based experiments. We first analyzed the LHCII complex reconstituted in membranes in dipolar-based ^{13}C-^{13}C (CC) and ^{15}N-^{13}C (NC) spectra, to verify the incorporation of isotope labels and to identify resonance signals of selective amino-acid and pigment types. Fig.2 presents the CC and NC spectra, showing that several amino-acid types can be identified based on their unique chemical-shift patterns. Helix and coil distributions can be distinguished for alanine, serine, threonine and glycine, as indicated [(29)], in agreement with the known crystallographic structure of plant LHCII that contains both helical stretches and large, coiled loops and tails. In addition to signals originating from the protein content, Chl and carotenoid signals can be identified in regions of the CC spectrum where no protein signals are expected, verifying that these components are also isotopically labeled. Remarkably, in the CC spectrum also a single set of lipid glycerol carbon resonances is observed. It is well-known that each monomer unit of LHCII contains one phosphatidyl-glycerol (PG) lipid, which forms the ligand for Chl611 (nomenclature Liu et al. [(13)]) and we attribute the detected lipid resonances in the CC spectrum to the head carbons of LHCII-bound intrinsic PG lipid molecules that were isotope labeled and isolated together with the complex.

Comparison of LHCII structure and dynamics in reconstituted and in native thylakoid membranes: results from dipolar-based experiments

Dipolar-based CC spectra of native thylakoids were collected using parameters identical to those used for the isolated LHCII. Fig. 3A shows the CC spectrum of LHCII (black) overlaid with the thylakoid spectrum (red) in the aliphatic region. The strong overlap of the two spectra demonstrates, in agreement with the biochemical analysis of our samples, that the

most abundant signals in the thylakoid spectra arise from LHCII. Many of the additional peaks that are detected in the thylakoid spectrum can be attributed to lipid signals, confirming that isotope labels are also incorporated into the thylakoid lipids. In particular, multiple resonance signals between 70 and 80 ppm are detected (indicated in Fig.3A) that are attributed to lipid galactosyl heads. To have a closer view on the LHCII protein secondary structure in reconstituted and in native membranes, we used correlation signals of Ala, Thr and Ser amino-acid types as reporters for the protein fold. These residue types were chosen because of the clear spectral separation of Ala, Thr and Ser C_α-C_β correlation signals, and of the distribution of those amino acids along the polypeptide sequences involving both helical and coil regions. The insets of panel 3B, C and D show the Ala, Thr and Ser selective regions. The helical and coil signals fall into separate regions as indicated. To compare the experimental shift correlations with the LHCII structure, three steps were undertaken: (i) models were build for Lhcbm1 and Lhcbm2, the two most abundant polypeptides that form the LHCII trimers in *Cr*, based on the spinach and pea crystal structures; (ii) C_α and C_β chemical shifts predictions were generated from the Lhcbm1 and Lhcbm2 homology models using the program SHIFTX2 [(30)] and (iii) simulated CC correlations were generated from the predicted chemical shifts using FANDAS [(31)]. The resulting chemical shift predictions are overlaid in the inset spectra and shown as cyan and orange crosses. Fig. S2 presents the spectra of LHCII and thylakoids in the full aliphatic region, with the Lhcbm1 and Lhcbm2 chemical-shift predictions overlaid. The sequences of Lhcbm1 and Lhcbm2, presented in the lower panel in Fig.3 show that most of the residues are conserved among Lhcbm1 and Lhcbm2. In the Thr and Ser insets, those residues are labeled together. Their predicted shift correlations however do not fully overlap in the coil regions, because of small differences in the folds of the Lhcbm1 and Lhcbm2 models.

We compared the structure-based predicted shifts of Thr, Ser and Ala (cyan, orange) and their experimental peaks in the LHCII spectrum (in black). Interestingly, some of the LHCII peaks match closely with predicted correlations for non-conserved residues. For instance experimental peaks are observed that are close to the predictions of S18 and S221, which Ser are only found in Lhcbm2, indicating that signals of specific polypeptides can be distinguished. However, some of the other predicted signals are not matched by any experimental peak. Cross resonance signals might not be detected because of inefficient

cross polarization caused by residue dynamics, or might be shifted to a different spectral region. Both effects are indicators of flexible protein sites. We considered deviations between predicted (ω pred) and experimentally observed (ω exp) correlations significant if $\sqrt{[(\omega_1 \text{ exp} - \omega_1 \text{ pred})^2 + (\omega_2 \text{ exp}-\omega_2 \text{ pred})^2]} \geq 1.2$ ppm. Using this error margin for the predictions, we find that no experimental signals are observed in the LHCII spectrum within the predicted range for residues T16, T35, S110, T205 and T188 in Lhcbm1 and for T22, T38, S113 and T191 in Lhcbm2. In the LHCII NC spectrum, we observe additional anomalies for V106, I111 and T213 for Lhbm1, and for G20, I114, T191 and T216 for Lhcbm2 (Fig. S3) According to the LHCII crystal structures, none of these residues is in direct Van der Waals contact with pigment ligands, excluding that protein-pigment interactions cause chemical-shift anomalies. The lower panel in Fig.3 shows the Lhcbm1 structure in which residues with deviating shifts are highlighted in red, revealing that the N-terminal stretch at the stromal site and in the CE loop, the edge of helix A, and the C terminus facing the lumen contains flexible protein sites.

J-based experiments reveal reduced LHCII dynamics in native membranes

Comparing the thylakoid spectrum to the LHCII spectrum in the Thr, Ser and Ala regions, several differences are observed. Some of the signals are shifted, and overall more cross peaks are observed in the Thr and Ser coil regions, stronger signal intensities are observed and better overlap between the experimental and predicted LHCII correlations. The enhanced signal intensities are indicative of improved cross-polarization efficiencies, suggesting that the thylakoid membrane is more rigid than the reconstituted membrane and causes reduced dynamics in LHCII. To test this hypothesis, we proceeded with *J*-based (INEPT-TOBSY) experiments that are selective for molecules with strong dynamics and large-amplitude motions, such as disordered segments. Fig. 4 presents the 2D INEPT-TOBSY spectrum of LHCII (black) overlaid on the INEPT-TOBSY spectrum of thylakoid membranes (red). As expected by the fact that the majority of the protein signals are visible in dipolar-based experiments, only limited sets of protein signals are detected in the *J*-based spectra that we refer to as *"J"* amino acids. The overlaid spectra clearly show that several *J* amino-acid residues are detected in the *J*-based spectrum of LHCII, whereas only few residues are

detected in the *J*-based spectrum of thylakoids, indeed showing a reduced dynamics in the thylakoid membrane environment.

We could assign the *J* residues in the LHCII spectrum to Ala, Thr, Ser, Phe, Pro, Val, Lys, Ile, Glu, Asn and Leu amino acid types (3xA,T,S and 1xF,P,V,K,I,E,N,L plus 1 L or D, see Table S1 and Fig.S4. Because these represent residues that display fast and large-amplitude motions, we predict that they are located in the non-helical loop stretches and in the terminal tails. The N terminus of Lhcbm2/7 (AAI, first three amino acids) and the C-terminal stretch of Lhcbm1 starting from A212 (ATKFTPQ) or the equivalent stretch in Lhcbm2/7 and Lhcbm3 (ATKFTPSA) contain many of the observed *J* amino-acid types. In addition, a Val *J* residue is observed. The only Val residues outside the helical regions are V106 in the BE loop of Lhcmb1 and V83 in the EC loop. V106 was indeed classified as a flexible residue based on analysis of the dipolar-based spectra. Interestingly, we observe three distinct sets of correlations for Ala, Thr and Ser residues, although the *J* amino acids can, on the basis of their C_α and C_β chemical shifts, all can be classified as having a random coil structure. A comparison with the predicted chemical-shift correlations (Fig. S5) shows that one of Thr *J* signals matches with predictions for T16 or T35/38 in the N-terminal stretch, for which no matching experimental shift was found in the dipolar-based CC spectrum. The Thr backbones in the N stretch might contain fast motions, but not adopt pure random coil structures because parts of the N stretch are constrained by intra-protein interactions. In summary, the analysis of the *J*-based LHCII spectrum indicates that fast-amplitude motions could occur for residues in the N- and C-terminus and/or for residues in the flexible BE or EC loops.

Remarkably, the *J*-based spectrum of LHCII also contains two sets of Chl signals that are assigned to P1, P2, P3, P3a and P4 phytol tail resonances (Table S2 and Fig.4, lower panel), indicating the presence of two Chl tails that exhibit strong dynamics. Resonance signals of the Chl phytol chains further towards the tail fall into the aliphatic region (10-30 ppm) and overlap with lipid CH_2 signals. In the LHCII crystal structures, the phytol chain structures of Chl*b* 605 and 606 (nomenclature according to Liu et al. [13]) are not observed, while the other Chl phytol tails are resolved and are involved in stabilizing pigment-protein interactions within the complex. Therefore, we conclude that the observed two sets of Chl phytol resonances in the *J*-based LHCII spectrum can be attributed to the dynamic tails of Chls 605 and 606 that are also close to flexible protein sites. Notably, the N-terminal region around

T16, G20 and the C terminus stabilize Chl601 and the xanthophyll-cycle carotenoid Vio or Zea as shown in Fig.5, and flexibility of those sites explains that carotenoids in this binding site are loosely bound and easily lost in isolated LHCII. Moreover, the region around T35 contains the binding pocket of Lutein 2 and could influence the dynamics of this carotenoid and its interaction with Chl601.

Most of of the amino-acid signals that are observed in the LHCII *J*-based spectrum, and the signals of the two Chl tails, are not observed in the thylakoid spectrum. This shows that the fast-amplitude motions in LHCII are significantly surpressed in the thylakoid membrane environment. We conclude that both small-amplitude thermal motions and large-amplitude segmental motions in LHCII complexes are significantly reduced in the native thylakoid membranes. The organization of LHCII in Photosystem II-LHCII (PSII-LHCII) supercomplexes, and the occurence of membrane stacks inside the thylakoids that are not mimicked in the proteoliposomes might well be the cause of its restrained dynamics in thylakoids. In contrast to the proteoliposome preparations, thylakoid membranes of *Cr* form stacks of 2-3 membrane layers that are stabilized by transversal salt bridges between the stromal sites of LHCII complexes, and are mediated by divalent cations [(32)]. Furthermore, specific arrangements of the super complexes occur in the lateral plane of the membrane. According to the cryo-electron microscopy (cryo-EM) structures of *spinach* PSII-LHCII super complexes, LHCII Chl605 and the protein AC and EC loops are in close contact with the minor antenna proteins CP29 or CP26 [(17, 33)] and also in the low-resolution structures of *Cr* PSII-LHCII, LHCII trimers are arranged next to CP29 and CP26 [(26)].

Dynamics of intrinsic lipids

A specific set of lipid signals was identified in the dipolar-based CC spectra (Fig.3) were attributed to PG, indicating that this lipid is strongly bound. LHCII complexes bind one PG lipid per monomer that is essential for ligating Chl611. Together with Chl612 and Chl610, these Chls form the terminal emitter domain of LHCII where excitations accumulate via downhill intra-protein energy-transfer. In the dissipative state, this site has been proposed as the quenching domain [(18)]. In the *J*-based CC spectra, multiple lipid signal resonances are observed in the thylakoid spectrum as well as in the LHCII spectrum. Resonances of lipid

galactosyl heads are observed in the region between 50-106 ppm that can be assigned to MGDG and a DGDG lipid molecules [34] and are summarized in Table S3. The reconstituted membranes in the LHCII sample are not isotope labeled and the probability of detecting ^{13}C-^{13}C cross correlations of natural-abundance carbons is very low. The lipid signals that are detected for isolated LHCII therefore must originate from intrinsic lipids that remained associated with the protein complex during the isolation procedure. However, their observation in the *J*-based spectrum indicates that that those lipids are very mobile and suggests that they have exchanged with the liposome bulk lipids after reconstitution of LHCII in the liposomes. The observed high mobility of the MGDG head atoms does not support the hypothesis of Seiwert et al., who suggested that specific hydrogen-bonding interactions might occur between LHCII and the MGDG galactosyl heads [35]. For the thylakoid sample, resonances of different lipid types are detected in *J* as well as dipolar-based spectra, showing the presence of both mobile and immobilized lipid molecules, in agreement with the results from our recent 1D MAS NMR studies on whole thylakoids and on intact cells [27] [36]. Signals from the unsaturated glycolipid tails, resonating between 20-35 ppm in ω_1 and between 130-137 ppm in ω_2, however, only appear in the INEPT spectrum. Seemingly, the unsaturated lipid chains are all mobile and disordered, despite the overall rigidity of the thylakoid membrane.

Implications for the LHCII conformational switch in vivo

The NMR analysis shows that in membranes *in vivo* at ambient temperature the conformational dynamics of LHCII are much more constrained than in thylakoid-mimicking environments *in vitro* and that both fast, segmental, and slower, thermal motions are suppressed. These findings call to question whether or not spontaneous fluctuations of individual LHC proteins between different conformational states, as has been observed by single-molecules spectroscopy (SMS) and has been suggested by MD simulations, do occur *in vivo*. With SMS, dynamic transitions were detected for isolated LHCII and conformational fluctuations under those conditions were strong enough to occasionally cross the energetic barriers between different conformational states. In vivo, it is more likely that the LHCs are

locked in their specific states and an actinic response is required that temporarily reduce the energetic barriers by alterations in the physicochemical environment.

Conclusion

We demonstrated the ability to detect the conformational dynamics of LHCII inside native membrane environments and conclude that the dynamics of LHCII in thylakoids is significantly restrained compared to its dynamics in reconstituted membranes. Notably, the thylakoid sample was isolated from cells grown under moderate light conditions and we assume that the thylakoid-embedded LHCII structures represent the light-harvesting conformation. Thus far this conformational state could only be studied *in vitro* using isolated proteins in detergent solutions [(3, 4, 8)] of which the dynamic features are not representative of their native states. Moreover, NMR spectroscopy can detect signals from different Lhcbm polypeptide types, which are not distinguished in crystallographic and cryo-EM structures. Selective Lhcbm mutants could be used in the future to further identify chemical shift contributions of the different polypeptide types [(37)]. Photosynthetic regulatory processes such as state transitions and NPQ are studied on thylakoid membranes, cells, or leaves under physiological conditions, whereas structural dynamics of the involved proteins has only been investigated on isolated complexes. The possibility to detect LHCII NMR chemical-shift signals in intact thylakoid membranes, and simultaneously detect the thylakoid membrane lipids, now opens a route to study the effects of thylakoid plasticity on the intrinsic protein conformational dynamics and states.

Material and Methods

Biosynthetic isotope labeling of Cr *cells and sample preparation*

For the experiments on isolated LHCII trimers, *Cr* cells from strain *cw15* were cultivated in Erlenmeyer flasks with liquid tris-acetate phosphate (TAP) medium, at 100 rpm agitation and 21 °C in a growth chamber. For optimal labeling of the LHCII complexes, cells were grown under mixotrophic conditions under dim light to minimize the uptake of $^{12}CO_2$ from air. Continuous illumination was provided from cool-white fluorescent lamps under low (< 25

µmoles photons m^{-2} s^{-1}) photosynthetically active radiation (400-700 nm). The TAP medium [38] used to grow labeled cells, was prepared using ^{13}C labeled sodium acetate (Sigma-Aldrich) and ^{15}N labeled ammonium chloride (Sigma-Aldrich). Cultures in labeled medium were set up starting from an optical density at 750 nm (OD_{750}) equal to 0.1 and were grown until OD_{750} = 1. Three rounds of cultivation in labeled medium were performed to ensure > 95 % labeling of the cells with ^{13}C and ^{15}N atoms. For experiments on whole fresh thylakoids, *Cr* cells were cultivated in TAP medium using ^{13}C labeled sodium acetate in a home-built photo chamber, under continuous illumination with cool white LEDs (~50 µmol m^{-2} s^{-1}). Cells were harvested in the exponential growth phase. The thylakoid and LHCII isolation procedures are described in the Suppementary Information. For the LHCII sample, 18 ml of LHCII in liposomes, containing approximately 20 mg LHCII and 1.5 mg Chl (as determined by OD_{680} of the Chls), was pelleted by ultra-centrifugation (223 000 g, 4 ^{o}C, 90 min) and transferred to a thin-wall 3.2 mm solid-state NMR MAS (Magic Angle Spinning) rotor through centrifugation. For the thylakoid sample, 12 ml of fresh thylakoid membrane containing 2 mg Chl and approximately 10 times more in protein content was pelleted by ultra-centrifugation (100 000 g, 4 ^{o}C, 45 min) and transferred to a thin-wall 3.2 mm MAS rotor.

Gel electrophoresis

Coomassie-stained SDS-page was performed using 15% Tris-glycine gels [39]. Samples were solubilized with a solubilization buffer (4 ×) containing 30% glycerol, 125 mM Tris pH 6.8, 0.1 M dithiothreitol, 9% SDS.

Solid-state NMR experiments

Solid-state NMR spectra of *U*-^{13}C-^{15}N LHCII in proteoliposomes and of ^{13}C-enriched thylakoid membranes were recorded on an ultra-high field 950-MHz ^{1}H Larmor frequency spectrometer (Bruker, Biospin, Billerica) equipped with a triple-channel ^{1}H, ^{13}C, ^{15}N 3.2 mm MAS probe. Typical π/2 pulses were 3 µs for ^{1}H, 5 µs for ^{13}C, and 8 µs for ^{15}N. The $^{1}H/^{15}N$ and $^{1}H/^{13}C$ cross-polarization (CP) [40] contact times were 800 µs and 1 ms, respectively, with a constant radio frequency (rf) field of 35 and 50 kHz on nitrogen and carbon, respectively,

while the proton lock field was ramped linearly around the n = 1 Hartmann/Hahn condition [41].The $^{15}N/^{13}Ca$ SPECIFIC-CP transfer [42] was implemented with an optimized contact time of 4.2 ms with a constant lock field of $2.5\times\nu_r$ applied on ^{15}N, while the ^{13}C field was ramped linearly (10% ramp) around $1.5\times\nu_r$. ^{1}H decoupling during direct and indirect acquisition was performed using SPINAL64 [43] with ~83 kHz irradiation. The presented 2D ^{13}C-^{13}C PARIS [44] spectra were collected with a mixing time of 30 ms at 17 kHz MAS at a set temperature of -18 ^{o}C. The 2D NCA and NCACX experiments [45] were performed on the LHCII sample at 14 kHz MAS frequency and a readout temperature of -18 ^{o}C. For the NCACX experiment a PARIS mixing time of 50 ms was used. The *J*-coupling based 2D ^{13}C-^{13}C INEPT-TOBSY[46, 47] experiments were recorded at -3 ^{o}C with TOBSY mixing of 6 ms at 14 kHz MAS. Spectra were processed with Bruker TopSpin 3.2 (Bruker, Germany) with LPfr linear prediction and fqc mode for Fourier transformation. Spectra were analyzed by Sparky version 3.114 [48] and MestReNova 11.0 (Mestrelab Research SL, Santiago de Compostela, Spain).

NMR chemical shift prediction using a plant-LHCII homology model

Homology models of *Cr* LHCII were built using the SWISS model web server [49] based on the LHCII crystal structure of spinach and using the Lhcmb1 or Lhcbm2 sequence of *Cr* LHCII [50]. The Lhcbm sequences and respective PDB models were used as input for SHIFTX2 [30] in order to predict the ^{13}C and ^{15}N chemical shifts. ^{13}C-^{13}C predicted correlation spectra for use in Sparky[48] were generated by FANDAS [31].

References

1. Kirchhoff, H. (2014) Structural changes of the thylakoid membrane network induced by high light stress in plant chloroplasts, *Philosophical Transactions of the Royal Society B: Biological Sciences 369*, 20130225.
2. Horton, P., and Ruban, A. (2005) Molecular design of the photosystem II light-harvesting antenna: photosynthesis and photoprotection, *Journal of Experimental Botany 56*, 365-373.
3. Ruban, A., Berera, R., Ilioaia, C., van Stokkum, I. H. M., Kennis, J. T. M., Horton, P., van Grondelle, R., Pascal, A., van Amerongen, H., and Robert, B. (2007) Identification of a mechanism of photoprotective energy dissipation in higher plants, *Nature 450*, 575-578.
4. Kruger, T., Ilioaia, C., Johnson, M., AV Ruban, Papagiannakis, E., Horton, P., and Grondelle, R. v. (2012) Controlled Disorder in Plant Light-Harvesting Complex II Explains Its Photoprotective Role, *Biophysical journal 102*, 2669-2676.
5. Holt, N., Zigmantas, D., Valkunas, L., Li, X., Niyogi, K., and Fleming, G. (2005) Carotenoid cation formation and the regulation of photosynthetic light harvesting, *Science (New York, N.Y.) 307*, 433-436.
6. Robert, B., Horton, P., Pascal, A., and Ruban, A. (2004) Insights into the molecular dynamics of plant light-harvesting proteins in vivo, *Trends in plant science 9*, 385-390.
7. Schlau-Cohen, G. S., Yang, H.-Y., Krüger, T. P. J., Xu, P., Gwizdala, M., van Grondelle, R., Croce, R., and Moerner, W. E. (2015) Single-Molecule Identification of Quenched and Unquenched States of LHCII, *The Journal of Physical Chemistry Letters 6*, 860-867.
8. Pandit, A., Reus, M., Morosinotto, T., Bassi, R., Holzwarth, A., and Holzwarth, A. R. (2013) An NMR comparison of the light-harvesting complex II (LHCII) in active and photoprotective states reveals subtle changes in the chlorophyll a ground-state electronic structures, *Biochimica et biophysica acta. Bioenergetics 1827*, 738-744.
9. Liguori, N., Periole, X., Marrink, S. J., and Croce, R. (2015) From light-harvesting to photoprotection: structural basis of the dynamic switch of the major antenna complex of plants (LHCII), *Sci Rep 5*, 15661.
10. Standfuss, A. C., Terwisscha van Scheltinga, M., Lamborghini, W., and Kühlbrandt. (2005) Mechanisms of photoprotection and nonphotochemical quenching in pea light-harvesting complex at 2.5 Å resolution, *EMBO journal 24*, 919-928.
11. Papadatos, S., Charalambous, A. C., and Daskalakis, V. (2017) A pathway for protective quenching in antenna proteins of Photosystem II, *Scientific Reports 7*, 2523.
12. Miloslavina, Y., Wehner, A., Lambrev, P. H., Wientjes, E., Reus, M., Garab, G., Croce, R., and Holzwarth, A. R. (2008) Far-red fluorescence: A direct spectroscopic marker for LHCII oligomer formation in non-photochemical quenching, *FEBS Letters 582*, 3625-3631.
13. Liu, Z., Yan, H., Wang, K., Kuang, T., Zhang, J., Gui, L., An, X., and Chang, W. (2004) Crystal structure of spinach major light-harvesting complex at 2.72 Å resolution, *Nature 428*, 287-292.
14. Fehr, N., Dietz, C., Polyhach, Y., von Hagens, T., Jeschke, G., and Paulsen, H. (2015) Modeling of the N-terminal Section and the Lumenal Loop of Trimeric Light Harvesting Complex II (LHCII) by Using EPR, *J Biol Chem 290*, 26007-26020.
15. Crisafi, E., and Pandit, A. (2017) Disentangling protein and lipid interactions that control a molecular switch in photosynthetic light harvesting, *Biochim Biophys Acta 1859*, 40-47.
16. Natali, A., Gruber, J. M., Dietzel, L., Stuart, M. C., van Grondelle, R., and Croce, R. (2016) Light-harvesting Complexes (LHCs) Cluster Spontaneously in Membrane Environment Leading to Shortening of Their Excited State Lifetimes, *J Biol Chem 291*, 16730-16739.
17. Wei, X., Su, X., Cao, P., Liu, X., Chang, W., Li, M., Zhang, X., and Liu, Z. (2016) Structure of spinach photosystem II–LHCII supercomplex at 3.2 Å resolution, *Nature 534*, 69.
18. Ruban, A. V., Johnson, C. D. P., and Duffy. (2012) The photoprotective molecular switch in the photosystem II antenna, *Biochimica et biophysica acta. Bioenergetics 1817*, 167-181.

19. Ward, Meaghan E., Wang, S., Munro, R., Ritz, E., Hung, I., Gor'kov, Peter L., Jiang, Y., Liang, H., Brown, Leonid S., and Ladizhansky, V. (2015) In Situ Structural Studies of Anabaena Sensory Rhodopsin in the E. coli Membrane, *Biophysical Journal 108*, 1683-1696.
20. Miao, Y., Qin, H., Fu, R., Sharma, M., Can, T., Hung, I., Luca, S., Gor'kov, P. L., Brey, W. W., and Cross, T. A. (2012) M2 Proton Channel Structural Validation from Full Length Protein Samples in Synthetic Bilayers and E. coli Membranes, *Angewandte Chemie (International ed. in English) 51*, 8383-8386.
21. Fu, R., Wang, X., Li, C., Santiago-Miranda, A. N., Pielak, G. J., and Tian, F. (2011) In situ structural characterization of a recombinant protein in native Escherichia coli membranes with solid-state magic-angle-spinning NMR, *Journal of the American Chemical Society 133*, 12370-12373.
22. Kaplan, M., Narasimhan, S., de Heus, C., Mance, D., van Doorn, S., Houben, K., Popov-Celeketic, D., Damman, R., Katrukha, E. A., Jain, P., Geerts, W. J. C., Heck, A. J. R., Folkers, G. E., Kapitein, L. C., Lemeer, S., van Bergen En Henegouwen, P. M. P., and Baldus, M. (2016) EGFR Dynamics Change during Activation in Native Membranes as Revealed by NMR, *Cell 167*, 1241-1251 e1211.
23. Renault, M., Pawsey, S., Bos, M. P., Koers, E. J., Nand, D., Tommassen-van Boxtel, R., Rosay, M., Tommassen, J., Maas, W. E., and Baldus, M. (2012) Solid-state NMR spectroscopy on cellular preparations enhanced by dynamic nuclear polarization, *Angew Chem Int Ed Engl 51*, 2998-3001.
24. Baker, L. A., Sinnige, T., Schellenberger, P., de Keyzer, J., Siebert, C. A., Driessen, A. J. M., Baldus, M., and Grunewald, K. (2017) Combined (1)H-Detected Solid-State NMR Spectroscopy and Electron Cryotomography to Study Membrane Proteins across Resolutions in Native Environments, *Structure (London, England : 1993)*.
25. Shi, P., Li, D., Chen, H., Xiong, Y., Wang, Y., and Tian, C. (2012) In situ (19)F NMR studies of an E. coli membrane protein, *Protein Science : A Publication of the Protein Society 21*, 596-600.
26. Drop, B., Webber-Birungi, M., Yadav, S. K. N., Filipowicz-Szymanska, A., Fusetti, F., Boekema, E. J., and Croce, R. (2014) Light-harvesting complex II (LHCII) and its supramolecular organization in Chlamydomonas reinhardtii, *Biochimica et Biophysica Acta (BBA) - Bioenergetics 1837*, 63-72.
27. Azadi Chegeni, F., Perin, G., Sai Sankar Gupta, K. B., Simionato, D., Morosinotto, T., and Pandit, A. (2016) Protein and lipid dynamics in photosynthetic thylakoid membranes investigated by in-situ solid-state NMR, *Biochim Biophys Acta 1857*, 1849-1859.
28. Ward, M. E., Ritz, E., Ahmed, M. A., Bamm, V. V., Harauz, G., Brown, L. S., and Ladizhansky, V. (2015) Proton detection for signal enhancement in solid-state NMR experiments on mobile species in membrane proteins, *J Biomol NMR 63*, 375-388.
29. Wang, Y., and Jardetzky, O. (2002) Investigation of the neighboring residue effects on protein chemical shifts, *Journal of the American Chemical Society 124*, 14075-14084.
30. Han, B., Wishart, D. S., Liu, Y., and Ginzinger, S. W. (2011) SHIFTX2: significantly improved protein chemical shift prediction, *J Biomol NMR 50*, 43-57.
31. Gradmann, S., Ader, C., Dittmann, M., Engelhard, M., Heinrich, I., Cukkemane, A., Baldus, M., Nand, D., Dijk, M. v., and Bonvin, A. M. J. J. (2012) Rapid prediction of multi-dimensional NMR data sets, *J Biomol NMR 54*, 377-387.
32. Sculley, M. J., Duniec, J. T., Thorne, S. W., Chow, W. S., and Boardman, N. K. (1980) The stacking of chloroplast thylakoids: Quantitative analysis of the balance of forces between thylakoid membranes of chloroplasts, and the role of divalent cations, *Archives of Biochemistry and Biophysics 201*, 339-346.
33. Su, X., Ma, J., Wei, X., Cao, P., Zhu, D., Chang, W., Liu, Z., Zhang, X., and Li, M. (2017) Structure and assembly mechanism of plant C2S2M2-type PSII-LHCII supercomplex, *Science (New York, N.Y.) 357*, 815-820.

34. de Souza, L. M., Iacomini, M., Gorin, P. A., Sari, R. S., Haddad, M. A., and Sassaki, G. L. (2007) Glyco- and sphingophosphonolipids from the medusa Phyllorhiza punctata: NMR and ESI-MS/MS fingerprints, *Chem Phys Lipids 145*, 85-96.
35. Seiwert, D., Witt, H., Janshoff, A., and Paulsen, H. (2017) The non-bilayer lipid MGDG stabilizes the major light-harvesting complex (LHCII) against unfolding, *Scientific Reports 7*, 5158.
36. Azadi-Chegeni, F., Schiphorst, C., and Pandit, A. (2018) In vivo NMR as a tool for probing molecular structure and dynamics in intact Chlamydomonas reinhardtii cells, *Photosynthesis Research 135*, 227-237.
37. Ferrante, P., Ferrante, P., Ballottari, M., Bonente, G., Giuliano, G., and Bassi, R. (2012) LHCBM1 and LHCBM2/7 Polypeptides, Components of Major LHCII Complex, Have Distinct Functional Roles in Photosynthetic Antenna System of Chlamydomonas reinhardtii, *Journal of biological chemistry 287*, 16276-16288.
38. Krishna K. Niyogi, O. B., and Arthur R. Grossman (1997) Chlamydomonas Xanthophyll Cycle Mutants Identified by Video Imaging of Chlorophyll Fluorescence Quenching *The Plat Cell 9*, 1369-1380.
39. Laemmli, U. K. (1970) Cleavage of Structural Proteins during the Assembly of the Head of Bacteriophage T4, *Nature 227*, 680-685.
40. A. Pinest, M. G. G., and J. S. Waugh. (1973) Proton-enhanced NMR of dilute spins in solids, *THE JOURNAL OF CHEMICAL PHYSICS 69*, 569-590.
41. Hartmann, S. R., and Hahn, E. L. (1962) Nuclear Double Resonance in the Rotating Frame, *Physical Review 128*, 2042-2053.
42. Baldus, M., Petkova, A. T., Herzfeld, J., and Griffin, R. G. (1998) Cross polarization in the tilted frame: assignment and spectral simplification in heteronuclear spin systems, *Molecular Physics 95*, 1197-1207.
43. B. M. Fung, A. K. K. a. K. E. (2000) An Improved Broadband Decoupling Sequence for Liquid Crystals and Solids, *Journal of Magnetic Resonance 142*, 97-101.
44. Weingarth, M., Demco, D. E., Bodenhausen, G., and Tekely, P. (2009) Improved magnetization transfer in solid-state NMR with fast magic angle spinning, *Chemical Physics Letters 469*, 342-348.
45. Baldus, M. (2002) Correlation Experiments for Assignment and Structure Elucidation of Immobilized Polypeptides Under Magic Angle Spinning, *Prog. Nucl. Magn. Reson. Spectr 1-47*.
46. Baldus, M., and Meier, B. H. (1996) Total Correlation Spectroscopy in the Solid State. The Use of Scalar Couplings to Determine the Through-Bond Connectivity, *Journal of Magnetic Resonance, Series A 121*, 65-69.
47. Gareth A. Morris, a. R. F. (1979) Enhancement of nuclear magnetic resonance signals by polarization transfer, *J. Am. Chem. Soc 101*, 760–762.
48. TD Goddard, D. K. SPARKY, *University of California, San Francisco*.
49. Arnold, K., Bordoli, L., Kopp, J., and Schwede, T. (2006) The SWISS-MODEL workspace: a web-based environment for protein structure homology modelling, *Bioinformatics 22*, 195-201.
50. Natali, A., and Croce, R. (2015) Characterization of the major light-harvesting complexes (LHCBM) of the green alga Chlamydomonas reinhardtii, *PLoS One 10*, e0119211.

Figure captions

Figure 1

A: LHCII protein structure.

B: LHCII structure including the pigments, with Chla in green, Chl*b* in blue, lutein in red and neoxanthin in purple and violaxanthin in yellow.

C: top view of a trimeric LHCII complex.

D: Sucrose gradient of *Cr* thylakoids after solubilizing with 0.6% α-DM, showing the fraction of trimeric LHCII.

E: SDS page gel analysis of the *Cr* thylakoid preparation and of isolated LHCII.

Figure 2

A-C: ^{13}C-^{13}C PARIS spectrum of membrane-reconstituted LHCII. Helix (h) and coil (c) C_α-C_β correlations of Thr, Ser and Ala and C_α -C correlations of Gly are indicated. In addition, protein correlations of Pro, Glu, Ile, and Val are indicated with black contour boxes. Chl, carotenoid and lipid correlations are indicated in respectively green, orange and blue. Their attributed carbon atom types are color-coded in the chemical structures in panel E.

D: ^{15}N-^{13}C NCACX spectrum of membrane-reconstituted LHCII. N-C_α correlations of Gly, Ser, Ala and Thr are indicated.

E: Chemical structures of Lutein, Chl*a* and of a glyco- or phospholipid molecule with the NMR detected atom types indicated.

Figure 3

Left: A; CP-PARIS spectrum of thylakoid membranes (red) with the LHCII spectrum (black) overlaid. The insets show the Ala (B), Thr (C) and Ser (D) spectral regions. In the insets, chemical-shift predictions of Lhcbm1 (cyan crosses) and Lhcbm2 (orange crosses) are

overlaid. The helix (h) and coil (c) regions are indicated ith black and red boxes. Predicted shifts that significantly deviate from experimental correlations in the LHCII spectrum are highlighted in red.

Lower panel: Lhcbm1 homology model and Lhcbm1 and Lhcbm2 sequences, highlighting in red and purple the residues which with chemical-shift deviations were observed in the CP-based LHCII CC (red) and NC (purple) spectra. Other Thr, Ser and Ala residues are indicated in blue in the structure.

Figure 4

Upper panel: Overlay of the INEPT-TOBSY spectrum of *Cr* LHCII (black) and of *Cr* thylakoids (red). Resonance signals of the two Chls, the lipids and Ala, Thr, Ser, and Phe are indicated. Lower panel: Chemical structure of MGDG lipid and Chl, highlighting the lipid and Chl atom types that are detected in the spectra.

Figure 5

LHCII pigment-protein crystal structure, highlighting flexible protein sites and pigments that are in close vicinity.

Figure 1

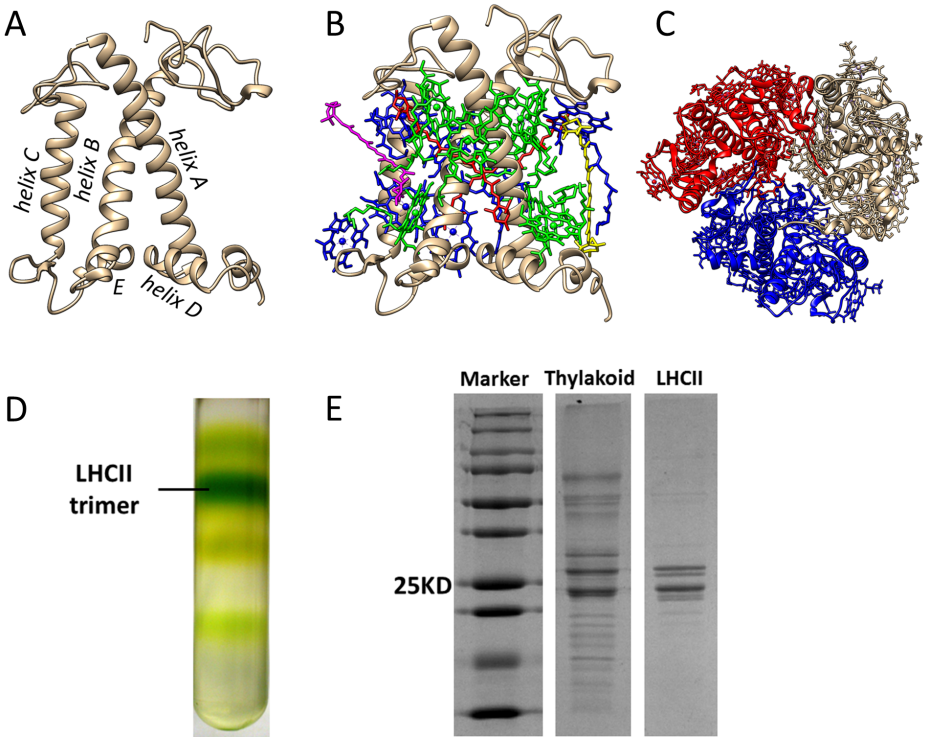
A
helix C
helix B
helix A
E
helix D
B
C
D
LHCII
trimer
E
Marker
Thylakoid
LHCII
25KD

Figure 2

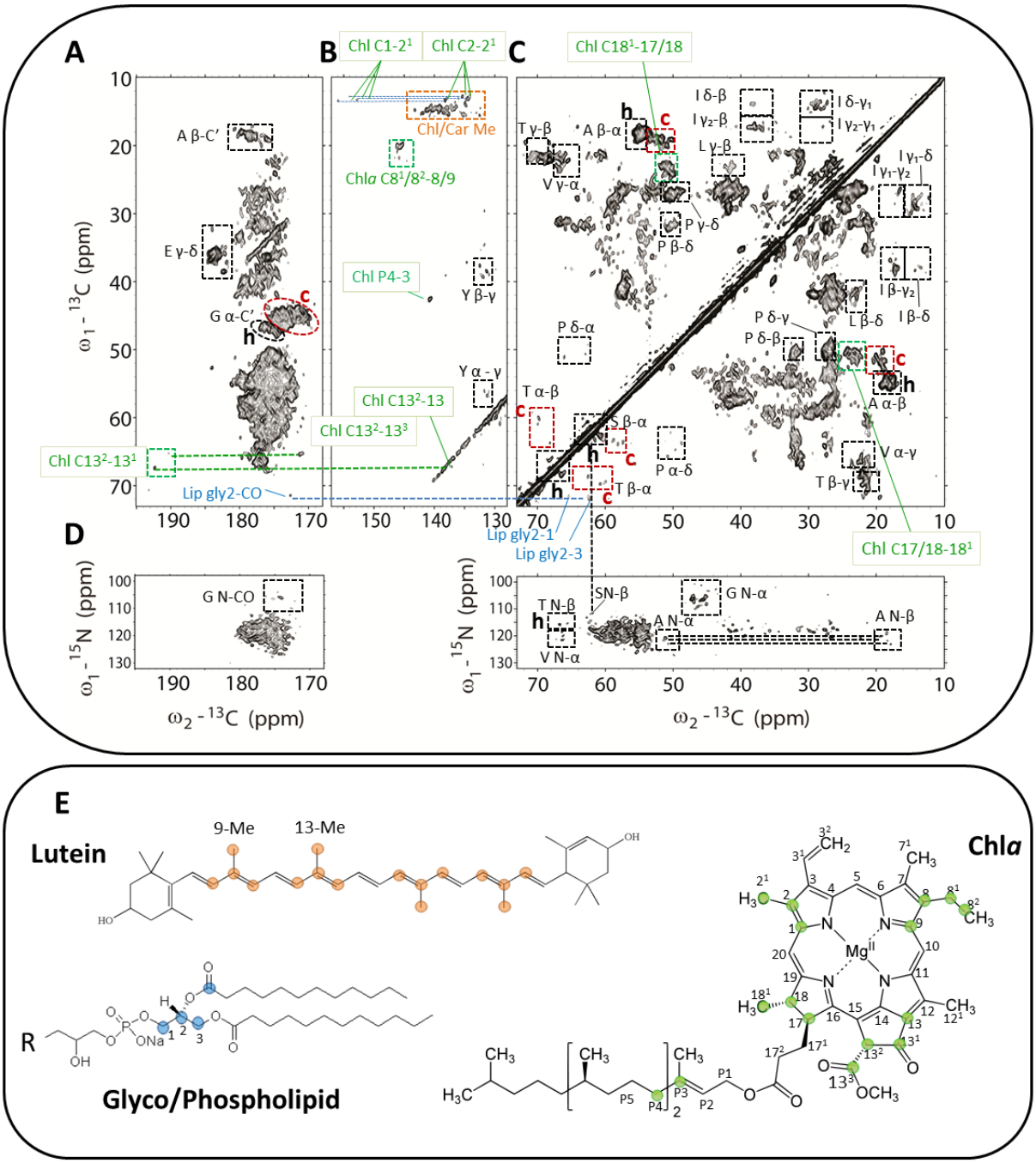
A
B
C
D
E
Chl C1-2¹
Chl C2-2¹
Chl/Car Me
Chla C8¹/8²-8/9
Chl P4-3
Chl C13²-13
Chl C13²-13³
Chl C13²-13¹
Lip gly2-CO
Chl C18¹-17/18
Chl C17/18-18¹
Lip gly2-1
Lip gly2-3
A β-C′
E γ-δ
G α-C′
Y β-γ
Y α-γ
T γ-β
A β-α
V γ-α
P γ-δ
P β-δ
I δ-β
I γ₂-β
L γ-β
I δ-γ₁
I γ₂-γ₁
I γ₁-δ
I γ₁-γ₂
I β-γ₂
I β-δ
L β-δ
P δ-α
P δ-γ
P δ-β
T α-β
S β-α
P α-δ
T β-α
A α-β
V α-γ
T β-γ
G N-CO
T N-β
SN-β
G N-α
A N-α
A N-β
V N-α
ω₁ - ¹³C (ppm)
ω₂ - ¹³C (ppm)
ω₁ - ¹⁵N (ppm)
Lutein
9-Me
13-Me
Chla
Glyco/Phospholipid

Figure 3

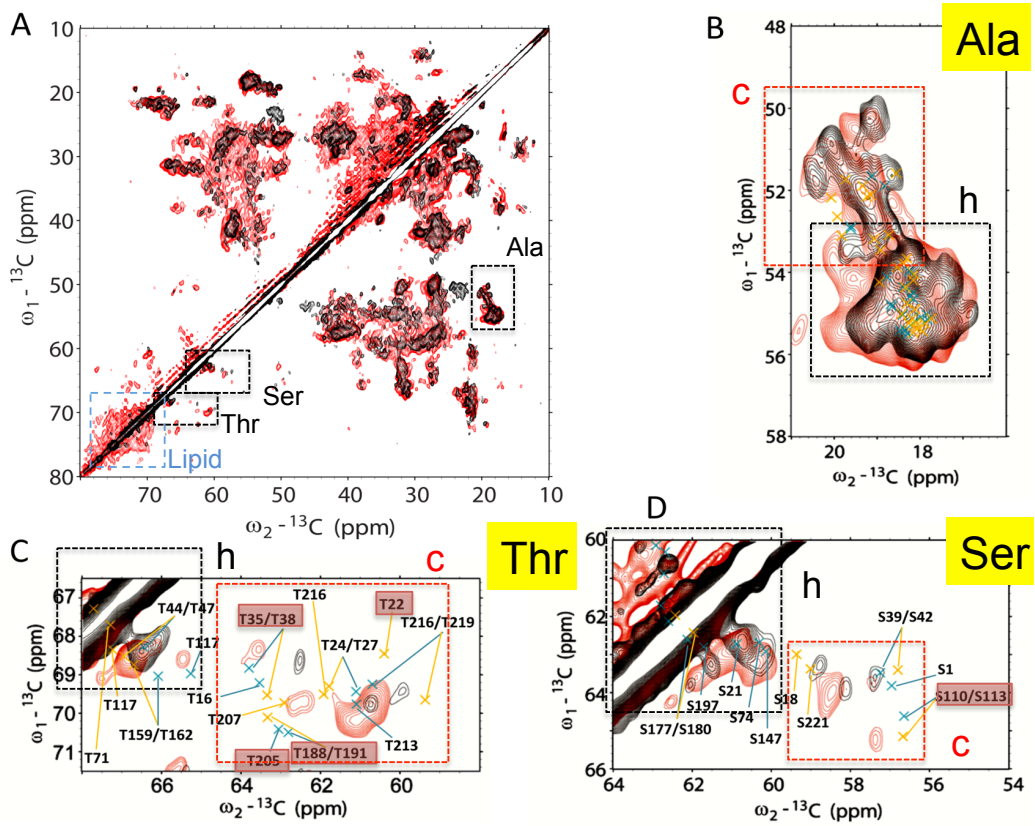


```
Lhcbm1      ---------VEARRTVKP--ASKASTPDSFWYGPERPLFLGAFT-GEPPSYLTGEFPGDY 31
Lhcbm2      -------------------------AAIEWYGPDRPKFLGPFSEGDTPAYLTGEFPGDY 34
                                      *:***:** :** :: .   *:**********
                                 Helix B                      Helix E
Lhcbm1      GWDTAGLSADPETFKRYRELELIHARWAMLGALGCIFPELLGSYGVPFGEAVWFKAGAQI 91
Lhcbm2      GWDTAGLSADPETFKRYRELELIHARWAMLGALGCITPELLAKNGIPFGEAVWFKAGAQI 94
            ************************************ ****.. *   *************
                                 Helix C
Lhcbm1      FQEGGLDYLGNPNLVHAQSILAILGTQVLLMGAIEGYRVNGGPLGEGLDKLYPGGSFDPL 151
Lhcbm2      FAEGGLNYLGNENLIHAQSIIATLAFQVVVMGLAEAYRANGGPLGEGLDPLHPGGAFDPL 154
            * ****:**** .*:***.*:* *.  **::**   *.**.**** ***** *:** :****
                        Helix A                      Helix D
Lhcbm1      GLADDPDTFAELKVKEIKNGRLAMFSMFGFFVQAIVTGKGPLQNLSDHLANPGTNNAFAY 211
Lhcbm2      GLADDPDTFAELKVKEIKNGRLAMFSMFGFFVQAIVTGKGPIQNLDDHLANPTAVNAFAY 214
            ****************************************:***.***:**  . ****:

Lhcbm1      ATKFTPQ- 218
Lhcbm2      ATKFTPSA 222
            ******.
```

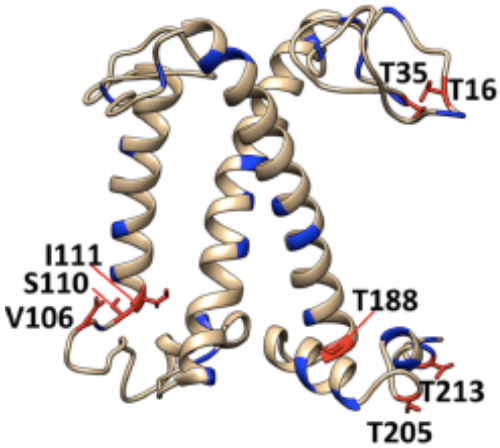

Figure 4

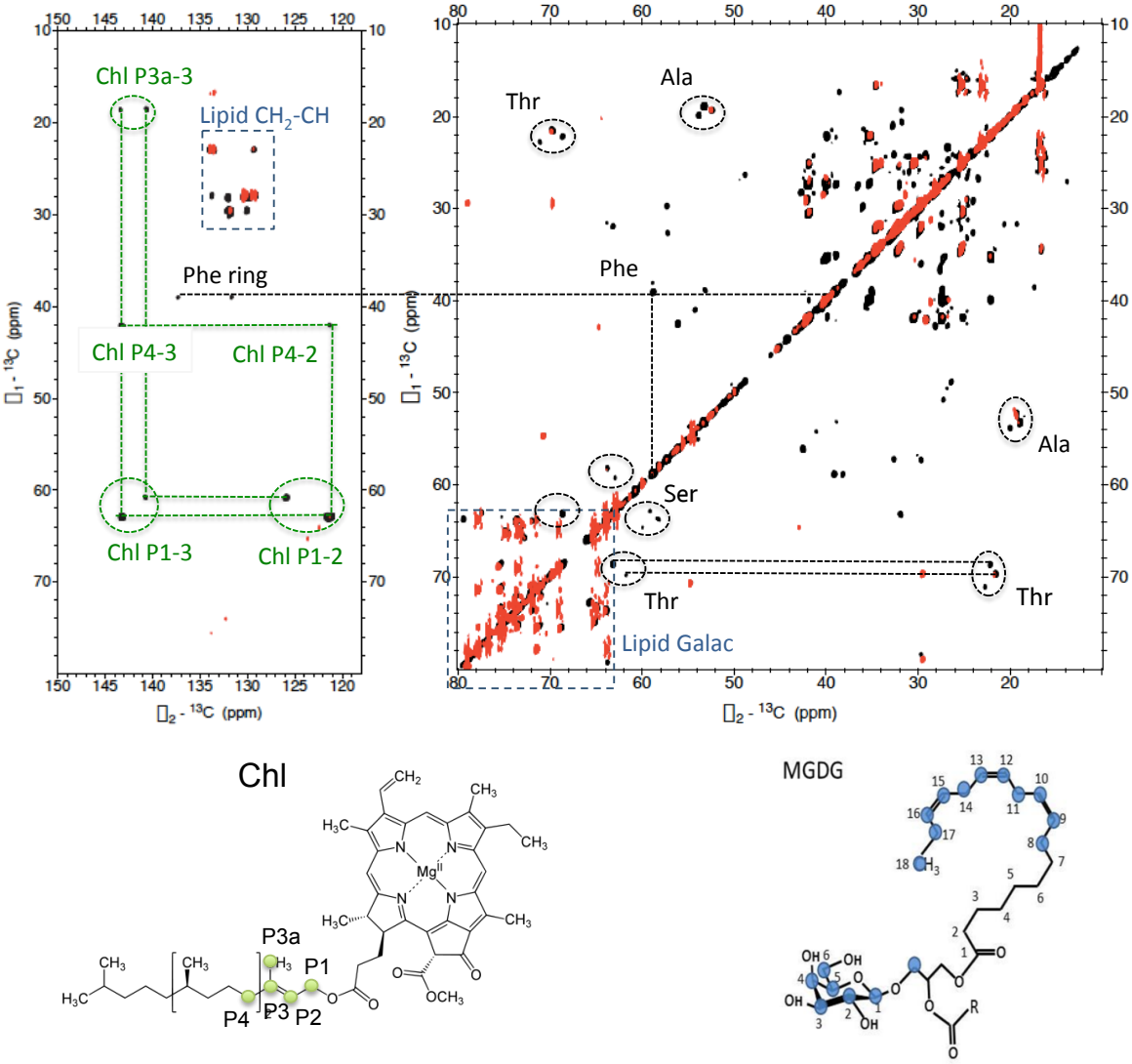
Chl P3a-3
Lipid CH2-CH
Phe ring
Chl P4-3
Chl P4-2
Chl P1-3
Chl P1-2
Thr
Ala
Phe
Ser
Ala
Thr
Thr
Lipid Galac
Chl
P3a
P1
P4
P3
P2
MGDG
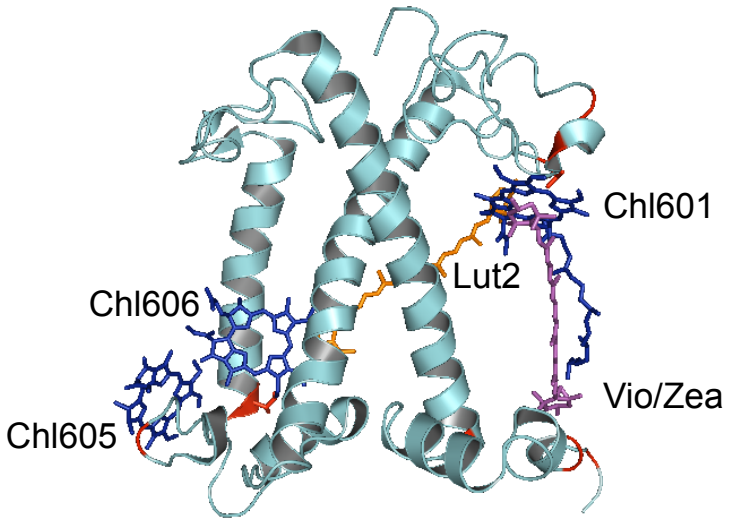
Figure 5